Macromolecules **1997,** *30,* 5753−5757

Interaction between Thiophene and Solvated Lewis Acids and the Low-Potential Electrochemical Deposition of a Highly Anisotropic Conducting Polythiophene Film

Shi Jin and Gi Xue*

Department of Chemistry, Institute of Coordination Chemistry, Nanjing University, Nanjing 210093, People's Republic of China

Received May 9, 1996; Revised Manuscript Received June 26, 1997[⊗]

ABSTRACT: Fourier transform Raman spectroscopy of a thiophene solution shows a reduction of aromaticity of the thiophene ring by the interaction with a solvated Lewis acid, which lowers the oxidation potential of the monomer. Low-potential electrochemical deposition of polythiophene was carried out in the presence of a Lewis acid in a solvent with a suitable donor number. High quality conducting polythiophene films were prepared at low potential in BF_3−ethyl ether. The conductivity parallel to the film surface is more than 10^4 times that across the film thickness. This anisotropy is related to the orientation of polythiophene chains. The molecular arrangement of polythiophene on a stainless steel electrode was investigated by surface-enhanced Raman scattering and infrared reflection−absorption spectroscopy.

Introduction

During the last 10 years electrically conducting polymers have received a great deal of attention due to their potential applications.[1−4] Among a number of conducting polymers, polythiophene (PT) has attracted much interest as it is stable to both oxygen and moisture.[5] Most conductive PT films were prepared by the electrochemical polymerization of thiophene in an organic solvent such as acetonitrile, nitromethane, nitrobenzene, or propylene carbonate.[6−8] However, electrooxidation of thiophene in these media requires potentials above 1.6 V vs SCE. The high potentials (above 1.45−1.55 V[9,10]) would irreversibly damage the conjugated system, due to overoxidation. Although thiophene oligomers can be polymerized at lower potentials, it must be emphasized that the resulting polymers show a lower average conjugation length when oligomers are used as starting molecules.[11−13]

In moderately concentrated $HClO_4$ (5 M) the polymerization of thiophene can take place at a very low potential (0.9 V vs SCE). However, the electrical conductivity of the resulting PT film is rather low (0.10−1 S cm^{-1}) compared with that obtained when the polymerization is carried out in organic media due to the decreased average length of conjugated segments evidenced by the hypochromic shift of the absorption maximum of the resulting polymer.[14]

Electrooxidation of benzene can be observed at a lower potential (1.6 V) in strong acidic media such as an $AlCl_3$/nitrobenzene solution than in liquid sulfur dioxide (2.1 V vs Ag/AgCl).[15−17] The significant decrease in the oxidation potential of benzene in the strong acidic media can be rationalized in two ways: first, benzene forms a complex with the strong acid, thereby reducing the resonance stabilization of the aromatic ring and shifting the oxidation potential to less anodic potential.[18] Second, the increased acidity of the solvent imparts a greater stability to the cation radical, which can promote the electrooxidative polymerization.

Nevertheless, thiophene is quite unstable in this strong acidic solvent and an acid-initiated additive polymerization takes place,[19,20] resulting in a nonconjugated polymer. This prevents the preparation of films with good conductivity in strong acidic solvents by electrochemical polymerization of thiophene.

Recently, we found that the oxidation potentials of thiophene in solvated Lewis acids were related to the aromaticity of the thiophene rings, by studying the Fourier transform Raman (FT-Raman) spectra. Low-potential polymerization of thiophene in BF_3−ethyl ether (BFEE) could be successfully performed using the solvated strong Lewis acids BF_3−ethyl ether (BFEE) and $AlCl_3/CH_3CN$. The obtained polymer from BFEE was characterized as a conducting film with long effective conjugated length and with mechanical properties, which exceed an aluminum metal sheet. Of particular interest is that the conductivity in the direction of the film plane is more than 10^4 times higher than that in the perpendicular direction. This anisotropic conductivity is related to the molecular orientation. Fourier transform surface-enhanced Raman scattering (SERS) and infrared reflection−absorption spectroscopy were used to characterize the molecular arrangement of PT chains on metal.

Experimental Section

Chemicals. Thiophene and BFEE were purified by distillation before use. Acetonitrile was successively refluxed with potassium permanganate and phosphoric anhydride and then distilled in the presence of anhydrous potassium carbonate. Nitromethane was distilled after reflux with concentrated sulfur acid. Anhydrous aluminum chloride was used as received. $AlCl_3/CH_3CN$ solutions were used at a concentrate of 3 mol L^{-1}.

Electrochemical Experiments. Electrochemical examinations and polymerization were performed in a one-compartment three-electrode cell with the use of a PARC M273 potentiostat under the control of a computer. To obtain a free-standing film, stainless steel sheets (1.5 × 7 cm^2) were employed as working electrodes and counter electrodes, which were polished with abrasive paper (1200 mesh) and diamond paste (1.5 μm), and were cleaned in an ultrasonic acetone bath before use. The galvanostatic method was used for electrochemical polymerization at a current density of 1 mA cm^{-2}, and the thickness of the deposited films was controlled by the electric charge passed during film growth. Electrochemical measurements were carried out with a platinum disc (diameter 0.5 mm), polished, and cleaned as mentioned above before each

---

* To whom correspondence should be addressed.

[⊗] Abstract published in *Advance ACS Abstracts,* August 15, 1997.

S0024-9297(96)00692-4 CCC: $14.00

experiment. All potentials were measured versus an Ag/AgCl (3.5 M KCl) reference. Each solution containing 0.1 mol L^{-1} thiophene was degassed by bubbling dry argon before the experiment and by maintaining a slight argon overpressure during the experiment.

Measurement of Electrical and Mechanical Properties. After being washed well by acetone, the polymer films were stripped from the electrodes and dried under vacuum at ambient temperature; the conventional four-electrode cell was utilized to measure electrical conductivity of the PT film. The tensile strength of the free-standing PT film was measured at a stretching rate of 5 cm min^{-1}.

Spectroscopy Experiment. A UV–visible spectrum was obtained from a PT film deposited onto an ITO (indium tin oxide coated optical glass) at a deposited charge of 100 mC cm^{-2} under a current density of 1 mA cm^{-2}. FT-Raman studies of thiophene solutions were carried out at a concentration of 1 mol L^{-1}. For IR measurements, the PT films deposited onto stainless steel electrodes had been dedoped with 20% ammonia, washed with distilled water and acetone, and dried under vacuum at 80 °C for 24 h before spectroscopic characterization. A electrochemically roughened Au disk (diameter 3 mm) was employed as the substrate in the SERS experiment. In each experiment, the PT layer was deposited onto the electrode at a current density of 1 mA cm^{-2} with 20 S. All Raman spectra were recorded with 1.064 μm excitation. Ir spectra were recorded under vacuum.

Results and Discussion

Low-Potential Polymerization and FT-Raman Studies of Thiophene in Solvated Lewis Acid. The donor number is a property indicating the strength of interaction between the solvent and the acceptor, i.e., the Lewis acid, and is of particular significance in evaluating the coordination-chemical reactions in solution. The interaction between the solvent and the Lewis acid increases with an increasing donor number of the solvent. Due to relative weak interaction between Lewis acid and solvent, solvated $AlCl_3$ (or BF_3) in nitromethane (donor number = 2.7)[21] can initiate the additive polymerization of thiophene, resulting in nonconjugated chains. When we selected CH_3CN (donor number = 14.1) and $(C_2H_5)_2O$ (donor number = 19.2)[21] as the solvent, the interaction between the solvent and the Lewis acid is somewhat increased. As a result, the acidity of these solvated Lewis acids becomes too weak to initiate the additive polymerization of thiophene. Additive polymerization is not expected in an electrochemical reaction since it would result in a nonconjugated chain. These solvated Lewis acids seem to be suitable for electrochemical polymerization because thiophene is quite stable in these media.

Due to its sensitivity to the carbon skeleton, FT-Raman spectroscopy is an effective technique for studying the interaction between the acceptor and donor. A spectrum subtraction technique was employed to study the interaction between thiophene and the solvated Lewis acid. The absorbance of solvent was subtracted from the spectrum of each electrolyte solution, and the resulting spectrum reveals the interaction between thiophene and the solvent. The difference spectra are shown in Figure 1B–1D. Figure 1A is the Raman spectrum of pure thiophene, which shows ring C–H stretching bands at 3109.3 and 3083.6 cm^{-1}, C=C and C–C stretching bands at 1407.0 and 1359.6 cm^{-1}, and C–H in-plane deformation at 1079.9 and 1033.5 cm^{-1}. The absorption bands at 833.6 and 605.8 cm^{-1} are attributed to the deformation vibration of the ring and C–S–C, respectively.[22] In an aromatic ring, the difference in bond length between the C=C and C–C is reduced due to conjugation. Furthermore, the force constant of a bond relates to its bond strength. Then the frequency difference indicating the difference of the bond force constant between the $\nu_{C=C}$ and ν_{C-C}, can be employed to evaluate the aromaticity of a thiophene ring. The decrease in aromaticity of thiophene in the solvated Lewis acids was evidenced by frequency changes in Figure 1B–1D and was expected to reduce the oxidation potentials. We verified this point experimentally.

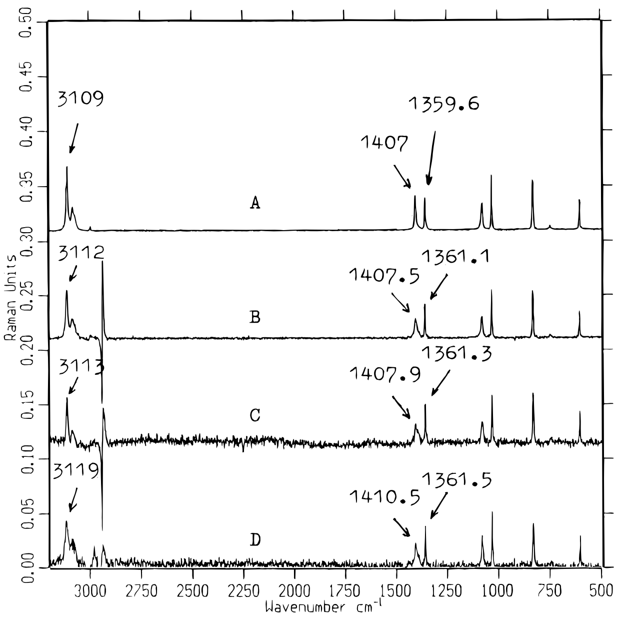

Figure 1. FT-Raman spectra of thiophene and thiophene in various solutions. (A) Raman spectrum of pure thiophene. (B)–(D) are the difference spectra subtracted corresponding solvents from the solutions: (B) Thiophene in CH_3CN; (C) thiophene in $AlCl_3/CH_3CN$; (D) thiophene in BFEE.

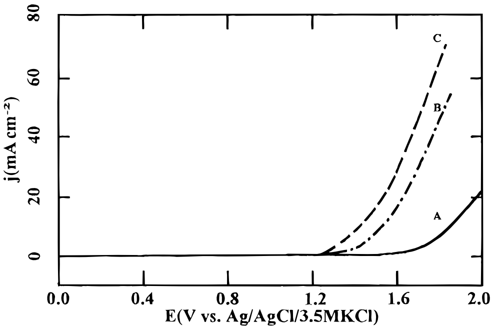

Figure 2. Anodic polarization curves of 0.1 mol L^{-1} $N(Et)_4ClO_4/CH_3CN$ (A), 3 mol L^{-1} of $AlCl_3/CH_3CN$ (B), and BFEE (C) at a scan rate of 10 mV S^{-1}. All solutions containing 0.1 mol L^{-1} of thiophene.

Figure 2 shows the anodic polarization curves of thiophene in various electrolyte solutions. The virgin oxidation of thiophene is initiated at 1.4 V in the presence of $AlCl_3$ (B), which has a lower anodic potential compared with that in the absence of the Lewis acid (A) (with a threshold potential of 1.7 V). Furthermore, the threshold potential of thiophene in BFEE solution (C) has a higher cathodic potential (1.3 V) than that in $AlCl_3/CH_3CN$ solution.

The frequency differences between C=C and C–C stretching lines in Figure 1 and the corresponding oxidation potential of thiophene in three solutions are listed in Table 1. It can be seen clearly that the aromaticity of a thiophene ring is reduced in the presence of a Lewis acid. The strength of interaction between thiophene and the solution increases in the

Table 1. Difference of Frequency between $\nu_{C=C}$ and ν_{C-C} and Oxidation Potential of Thiophene in a Corresponding Solution

solution	frequency difference ($\nu_{C=C} - \nu_{C-C}$) (cm^{-1})	oxidation potential (V)
CH_3CN	46.4	1.7
$AlCl_3/CH_3CN$	46.6	1.4
BFEE[a]	49.0	1.3

[a] BFEE: BF_3–ethyl ether.

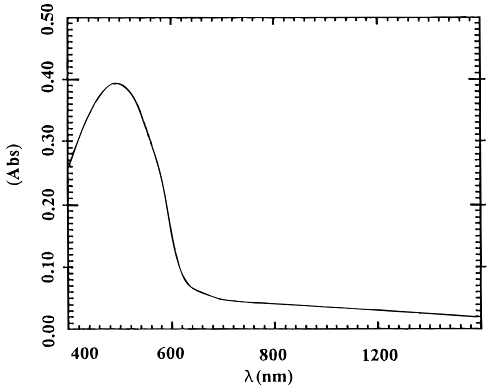

Figure 3. UV–vis spectrum of a dedoped PT film deposited onto an ITO electrode at a deposited charge of 100 mC cm^{-2}.

Table 2. Electrical and Mechanical Properties of PT Films Electropolymerized in Various Systems

solvent	conductivity (S cm^{-1})	tensile strength (MPa)	anisotropy[a] ($\sigma_{\parallel}/\sigma_{\perp}$)
CH_3CN	10	brittle	
BFEE	100	140	>10^4
$HClO_4$	0.1–1		

[a] The electrical conductivities for anisotropy calculation were measured using the two-electrode technique.

order of CH_3CN, $AlCl_3/CH_3CN$, and BFEE, which accords with their acidity order. With the increased interaction strength and decreased aromaticity, the oxidation potentials of thiophene in solvated Lewis acid are markedly lowered. The oxidation potentials of thiophene in $AlCl_3/CH_3CN$ and BFEE are 1.4 and 1.3 V, respectively, instead of 1.7 V in CH_3CN. It must be emphasized that these potentials are lower than the overoxidation potential of PT (1.45–1.55 V). In other words, high-quality PT film may be electrosynthesized in our systems. We prepared high-quality PT films with high conductivity, excellent tensile strength, and high anisotropy by electrooxidative polymerization of thiophene in BFEE.

Properties of Obtained Films

Compared with the films polymerized in $HClO_4$ at low potential, the average effective mean conjugation length of our polymers are rather high. The UV–visible spectrum of a dedoped PT film polymerized in 0.1 M thiophene/BFEE solution is shown in Figure 3. The adsorption maximum is at 500 nm instead of 460 nm of that prepared in $HClO_4$,[14] indicating higher conjugation in films prepared from the thiophene/BFEE system. Table 2 shows electrical and mechanical properties of PT films obtained in various systems. The conductivity data of the doped film agrees with the results of UV–visible analysis. A PT film prepared from the BFEE exhibits conductivity as high as 100 S cm^{-1}, while that obtained from the $HClO_4$ system has a lower conductivity in the range of 0.1–1 S cm^{-1}.[14] With the repression of overoxidation of deposited PT by the lower polymerization potentials, PT can be deposited onto the electrode more regularly and compactly, which results in high anisotropy and the compact morphology. Additionally, the repression of overoxidative degradation supports a large degree of polymerization. The transmission IR spectrum of a dedoped PT film shows a degree of polymerization of about 80 in contrast with about 40 in common media.[23] Furukawa et al. proposed the relationship[23,24]

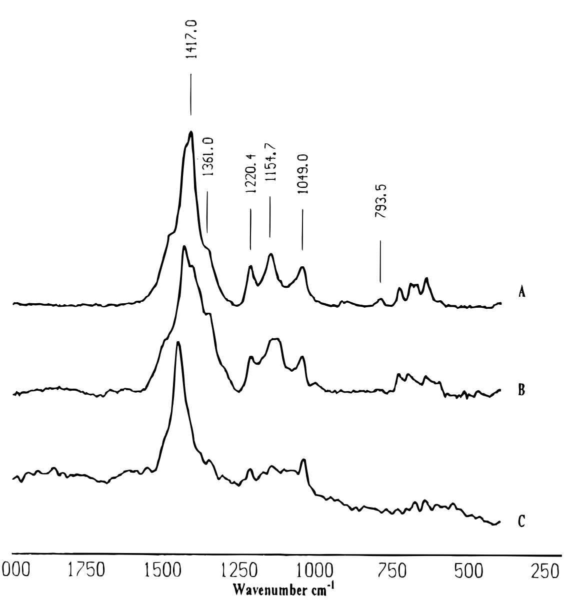

Figure 4. FT-Raman spectra of undoped polythiophene. (A) Surface-enhanced Raman spectrum of a thin layer PT film deposited onto a gold disk from 0.1 M thiophene/BFEE after the polymerization had proceeded for 20 s. (B) FT-Raman spectrum of a PT film deposited onto a gold disk from a 0.1 M thiophene/nitromethane solution. (C) FT-Raman spectrum of a PT film deposited onto ITO at a thickness of about 2 μm.

$$DP = 2(R_0/R + 2)$$

where R is the ratio of the integrated intensities of the two IR bands attributed to out-of-plane vibrations for monosubstituted (692 cm^{-1}) and 2,5-disubstituted (788 cm^{-1}) thiophenes. R_0 is the value of R estimated for the α,α′-sexithiophene. The free-standing polymer film prepared from thiophene/BFEE solution is flexible and has good mechanical properties. Its tensile strength (140 MPa) is greater than that of metal aluminum sheets (100–110 MPa). The extremely high tensile strength is a result of the large degree of polymerization and regular structure with compact morphology.

Orientation of PT Deposited onto the Surface of Stainless Steel. Our obtained PT films were characterized as two-dimensional conducting polymer films by their high anisotropy. This property is associated with the orientation of PT deposited onto the surface of an electrode. FT-Raman SERS and IR reflection–absorption spectroscopies are useful to study the orientation of molecules on the surface of metal. Figure 4A shows the FT-Raman SERS spectrum of a PT film deposited onto gold from a thiophene/BFEE solution after the polymerization had proceeded for 20 s. The corresponding SERS spectrum obtained from a thiophene/nitromethane solution was listed in Figure 4B for comparison. The normal FT-Raman spectra recorded from a PT film with a thickness of 2 μm deposited onto a ITO electrode are also illustrated in Figure 4C.

FT-Raman spectra in Figure 4A are not characterized as resonance Raman spectra because they were recorded by laser excitation at 1.064 μm while there is no absorption in this region for UV−visible spectra of PT. As can be seen in Figure 4A, the interaction with the surface caused a change in the spectrum. These changes include the marked bathochromic shift of C═C skeleton vibration (frequency shifted about 30 cm^{-1}), the appearance of new Raman lines, and changes in relative intensities of some Raman lines, compared with the normal Raman spectra of PT. These spectral changes along with the high signal-to-noise ratio in Figure 4A are characteristics of a typical SERS spectrum. In Figure 4A, the bands at 1417 and 1220 cm^{-1} are attributed to the ring C═C stretch and inter-ring C−C stretch,[25−27] respectively. C−H in-plane bending is found at 1049 cm^{-1}. ing-deformation vibrations appear at 734 and 692 cm^{-1}. The most interesting feature of the SERS of PT is the appearance of two new bands at 1155 and 794 cm^{-1}, arising from inter-ring C−C stretching vibrations of the distorted parts[26] and out-of-plane bending vibrations of βC−H,[27] respectively. The appearance of these bands indicates large enhancement of these bands in the SERS spectrum of Figure 4A.

A successful basis for analyzing SERS spectra with respect to orientation of adsorbates has been reported in the form of "surface selection rules" by Moskovits et al.[28−31] These rules are based on the electromagnetic theory of SERS intensity, which says that, via resonance interaction with surface plasmons of the metal, incident light increases in the electromagnetic fields which are most normal to the surface; normal modes of the adsorbed molecule involving changes in molecular polarizability with a component perpendicular to the surface are subject to the greatest enhancement.

On the basis of these surface selection rules for Raman spectroscopy and the relative intensity changes in Figure 4, the molecular arrangement of PT on stainless steel could be deduced. The polarizability moment change of $\gamma_{\beta\mathrm{C-H}}$ is perpendicular to the thiophene ring. This Raman inactive band becoming active in SERS implies a higher degree of ordering with the thiophene ring parallel to the metal surface for polymerization. Likewise, the polarizability moment change of distorted $\nu_{\mathrm{C-C\ inter-ring}}$ is not parallel but at an angle to the thiophene ring. The large enhancement of these two bands compared with normal Raman implies a higher degree of ordering with the thiophene ring parallel to the metal surface for polarization. The relatively strong band at 1155 cm^{-1} in Figure 4B which associates with the stretching mode of the C−C bond of distorted parts of the polymer implies that there are more distorted thiophene rings in PT prepared in thiophene/nitromethane solution, which results in less coplanarity. Additionally, a very weak out-of-plane bending band at 794 cm^{-1}, a strongly enhanced stretching vibration of an inter-ring C−C bond at 1361 cm^{-1}, and a much lower signal/noise ratio of Figure 4B than that of Figure 4A also suggest that PT film polymerized from the thiophene/BFEE solution has a much more ordered structure than that from the thiophene/nitromethane solution.

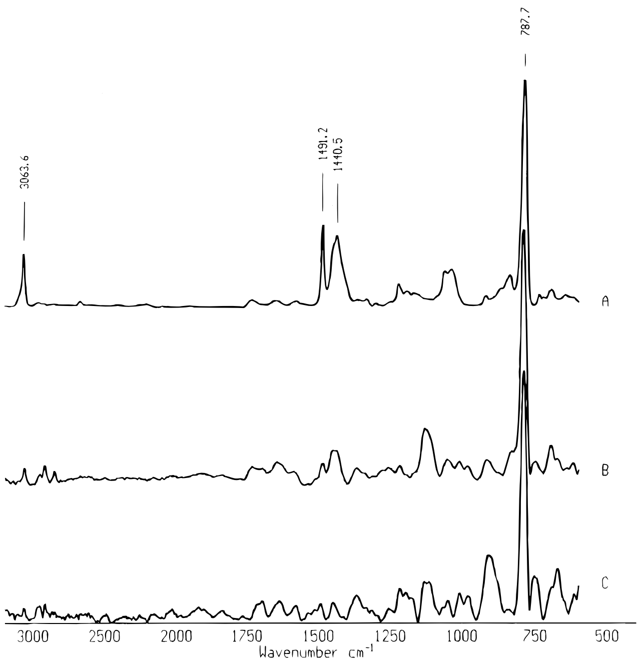

Figure 5. FT-IR spectra of PT. (A) Transmission IR of undoped PT films with a thickness of 10 μm. (B) Infrared reflection−absorption spectrum of a PT film deposited onto stainless steel at a thickness of 6000 Å. (C) Infrared reflection−absorption spectrum of a PT film deposited onto stainless steel at a thickness of 3000 Å.

Scheme 1. Arrangement of Polythiophene Chains on the Surface of an Electrode

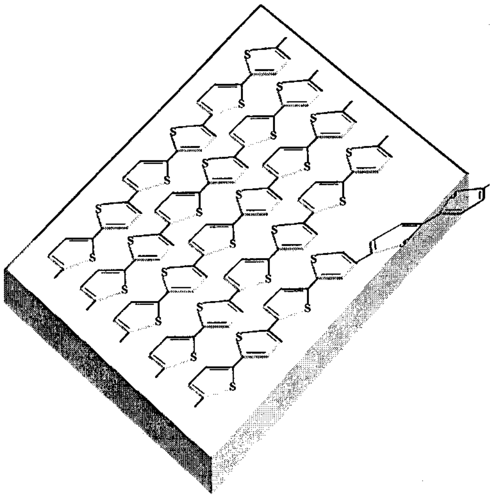

IR reflection−absorption PT on stainless steel supports the same conclusion. IR spectra of PT deposited onto stainless steel at a thickness of 3000 Å (B) and 6000 Å (C) are shown in Figure 5. A transmission IR of PT film is given for comparison (A). In spectrum A, absorptions at 3064, 1491, 1440, and 788 cm^{-1} are attributed to the $\nu_{\alpha\mathrm{C-H}}$, $\nu_{\mathrm{asC=C}}$, $\nu_{\mathrm{sC=C}}$, and $\gamma_{\beta\mathrm{C-H}}$,[23,25] respectively. The dipole moment change of $\nu_{\alpha\mathrm{C-H}}$, $\nu_{\mathrm{asC=C}}$, and $\nu_{\mathrm{sC=C}}$ are parallel to the thiophene ring, while that of $\gamma_{\beta\mathrm{C-H}}$ is perpendicular to the thiophene ring. According to the IR surface selection rule, the suppression of these modes parallel to the ring in spectra B and C strongly suggests that the rings of PT are parallel to the surface of the metallic electrode. A highly regular arrangement of PT chains can be observed at a thickness of 6000 Å on a stainless steel surface.

The results of SERS and IR reflection−absorption spectra suggest an orientation of PT deposited onto the surface of stainless steel by electrochemical polymerization as shown in Scheme 1 and can be described as follows: in the beginning of polymerization, the adsorbed thiophene rings were parallel to the surface of stainless steel due to the interaction between π-electrons of the aromatic ring and metal surface. The metal surface was coated with a layer of polymer in which the thiophene rings were parallel to the metal surface. The polymer was then oxidized to a positively charged form which will interact with π-electrons of successive monomer layers. When depositing layer-by-layer, very few defects formed in the polymer chains that acted as the distorted parts not coplanar to the conjugated segments. The high anisotropy in conductivity of the PT film is due to the regular molecular arrangement.

Conclusion

FT-Raman studies of thiophene in various solutions show that aromaticity of thiophene is somewhat reduced by the interaction with Lewis acid. Increasing the acidity of Lewis acid solution results in a decrease in the aromaticity of the thiophene ring and lowers oxidation potential of a monomer.

PT films deposited onto stainless steel in BFEE solution at low potentials are highly anisotropic and display high electrical conductivities and excellent mechanical properties. FT-Raman SERS and IR reflection−adsorption studies indicate that the thiophene rings of polymer chains are nearly parallel to the surface of the metal.

Acknowledgment. We are grateful for the financial support from the National Science Foundation of China and the Science Foundation of Jiangsu province.

References and Notes

(1) Tourillon, G.; Garnier, F. *J. Electroanal. Chem.* **1982**, *135*, 173.
(2) Yamamoto, T.; Wakayama, H.; Takahashi, F.; Takaki, K. *J. Phys. Chem.* **1992**, *96*, 8677.
(3) Downard, A. J.; Pletcer, D. *J. Electroanal. Chem.* **1986**, *206*, 147.
(4) Tourillon, G.; Garnier, F. *J. Phys. Chem.* **1983**, *87*, 2289.
(5) Garnier, F.; Tourillon, G.; Gazard, M.; Dubois, J. C. *J. Electroanal. Chem.* **1983**, *148*, 299.
(6) Diaz, A. F.; Logan, J. A. *J. Electroanal. Chem.* **1980**, *111*, 111.
(7) Sato, M.; Tanaka, S.; Kaerigama, K. *J. Chem. Soc., Chem. Commun.* **1985**, 713.
(8) Imanishi, K.; Satoh, M.; Yasuda, Y.; Tsushima, R.; Aoki, S. *J. Electroanal. Chem.* **1988**, *242*, 203.
(9) Krische, B.; Zagorska, M. *Synth. Met.* **1989**, *28*, C263.
(10) Gratzl, M.; Hsu, D.-F.; Riley, A. M.; Janata, J. *J. Phys. Chem.* **1990**, *94*, 5973.
(11) Roncali, J.; Garnier, F.; Lemaire, M.; Garreau, R. *Synth. Met.* **1986**, *15*, 323.
(12) Yumoto, Y.; Yoshimura, S. *Synth. Met.* **1985**, *13*, 185.
(13) Haviga, E. E.; Van Horssen, L. W. *Makromol. Chem. Makromol. Symp.* **1989**, *24*, 67.
(14) Bazzaoui, E. A.; Aeiyach, S.; Lacaze, P. C. *J. Electroanal. Chem.* **1994**, *364*, 63.
(15) Tsuchida, E.; Yamamoto, K.; Asada, T.; Nishide, H. *Chem. Lett.* **1987**, 1541.
(16) Yamamoto, K.; Asada, T.; Nishide, H.; Tsuchida, E. *Bull. Chem. Soc. Jpn.* **1988**, *61*, 1731.
(17) Hara, S.; Toshima, N. *J. Electroanal. Chem.* **1994**, *379*, 181.
(18) Andrew, L. J.; Keefer, R. M. *J. Am. Chem. Soc.* **1949**, *71*, 3644.
(19) Kovacic, P.; Mcfarland, K. N. *J. Polym. Sci., Polym. Chem. Ed.* **1979**, *17*, 1963.
(20) Margosian, D.; Kovacic, P. *J. Polym. Sci., Polym. Chem. Ed.* **1979**, *17*, 3695.
(21) Gutmann, V.; Schmied, R. *Coord. Chem. Rev.* **1974**, *12*, 263.
(22) Louarn, G.; Mevellec, J. Y.; Buisson, J. P.; Lefrant, S. *Synth. Met.* **1993**, *55−57*, 587.
(23) Furukawa, Y.; Akimoto, M.; Harada, I. *Synth. Met.* **1987**, *18*, 151.
(24) Sauvajol, J. L.; Chenouini, D.; Lere-Porte, J. P.; Chorro, C.; Moukala, B.; Petrissans, J. *Synth. Met.* **1990**, *38*, 1.
(25) Fujita, W.; Teramae, N.; Haraguchi, H. *Chem. Lett.* **1994**, *3*, 511.
(26) Bazzaoui, E. A.; Levi, G.; Aeiyach, S.; Aubard, J.; Marsault, J. P.; Lacaze, P. C. *J. Phys. Chem.* **1995**, *99*, 6628.
(27) Louarn, G.; Buisson, J. P.; Lefrant, S.; Fichou, D. *J. Phys. Chem.* **1995**, *99*, 11399.
(28) Suh, J. S.; Moskovits, M. *J. Am. Chem. Soc.* **1985**, *108*, 4711.
(29) Allen, C. S.; Van Duyne, R. P. *Chem. Phys. Lett.* **1979**, *63*, 45.
(30) Ni, F.; Cotton, T. M. *J. Raman Spectrosc.* **1988**, *19*, 429.
(31) Xue, G.; Lu, Y.; Zhang, J. *Macromolecules* **1994**, *27*, 809.

MA9606925